Results in Engineering 17 (2023) 100978

Contents lists available at ScienceDirect

Results in Engineering

journal homepage: www.sciencedirect.com/journal/results-in-engineering

Using an intelligent method for microgrid generation and operation planning while considering load uncertainty

Saeedeh Mansouri [a], Farhad Zishan [b,**], Oscar Danilo Montoya [c,d], Mohammadreza Azimizadeh [e], Diego Armando Giral-Ramírez [f,*]

[a] Department of Electrical and Computer Engineering, Babol Noushirvaniy University of Technology, Iran
[b] Department of Electrical Engineering, Sahand University of Technology, Tabriz, Iran
[c] Grupo de Compatibilidad e Interferencia Electromagnética, Facultad de Ingeniería, Universidad Distrital Francisco José de Caldas, Bogotá, 110231, Colombia
[d] Laboratorio Inteligente de Energía, Facultad de Ingniería, Universidad Tecnológica de Bolívar, Cartagena, 110231, Colombia
[e] Electrical Engineering Department, Amirkabir University of Technology, Tehran, Iran
[f] Facultad Tecnológica, Universidad Distrital Francisco José de Caldas, Bogotá, 110231, Colombia

ARTICLE INFO

Keywords:
Microgrid
Generation planning
Optimization problem
SALP Swarm algorithm
Operation cost
Uncertainty of generation and load

ABSTRACT

The integration of distributed generation (DG), energy storage systems (ESS), and controllable loads near the place of consumption has led to the creation of microgrids. However, the uncertain nature of renewable energy sources (wind and photovoltaic), market prices, and loads have caused issues with guaranteeing power quality and balancing generation and consumption. To solve these issues, microgrids should be managed with an energy management system (EMS), which facilitates the minimization of operating (performance) costs, the emission of pollutants, and peak loads while meeting technical constraints. To this effect, this research attempts to adjust parameters by defining indicators related to the best possible conditions of the microgrid. Generation planning, the storage of generated power, and exchange with the main grid are carried out by defining a dual-purpose objective function, which includes reducing the operating cost of power generation, as well as the pollution caused by it in the microgrid, by means of the SALP optimization algorithm. Moreover, in order to make the process more realistic and practical for microgrid planning, some parameters are considered as indefinite values, as they do not have exact values in their natural state. The results show the effect of using the introduced intelligent optimization method on reducing the objective function value (cost and pollution).

1. Introduction

Evaluating the capabilities of power systems with regard to supplying the network load at the permissible bus bar voltage and line loading values is one of power companies' primary goals. The constant change in system conditions due to various reasons and the increased influence of wind turbine production are highly effective on the correctness of judgments when it comes to planning the development of transmission systems. In this context, the use of approaches such as load flow is recommended as a suitable tool for analyzing systems under different operating conditions and as a suitable criterion power systems planning.

Considering the importance of the subject, random planning and microgrid performance in a short period of time in the distribution system can have effective results. Therefore, the functioning of the microgrid as an island, certainty and uncertainty is an important challenge for this purpose, by defining the parameters for the microgrid, it is tried to select the best mode by adjusting its parameters.

1.1. Literature review

In [1], an energy management system is proposed to optimize the microgrid (MG) performance in the short term while in the presence of random Renewable Energy Sources (RESs). In Ref. [2], energy management in MGs is performed while considering economic efficiency and environmental constraints, as well as improving reliability through 1) optimizing the type and capacity of Distributed Generation (DG) resources and Storage Devices (SDs), and 2) creating an Operational

* Corresponding author.
** Corresponding author.
E-mail addresses: saeede.mansoori@stu.nit.ac.ir (S. Mansouri), f_zishan99@sut.ac.ir (F. Zishan), odmontoyag@udistrital.edu.co (O.D. Montoya), azimizadeh.m@gmail.com (M. Azimizadeh), dagiralr@udistrital.edu.co (D.A. Giral-Ramírez).

https://doi.org/10.1016/j.rineng.2023.100978
Received 17 October 2022; Received in revised form 18 February 2023; Accepted 19 February 2023
Available online 22 February 2023

Nomenclature

MG	Miro Grid
RES	Renewable Energy Sources
DG	Distributed Generation
SD	Storage Device
OS	Operational Strategy
ESS	Energy Storage System
DER	Distributed Energy Resource
ARMIA	Auto Regressive Integrated Moving Average
EV	Electric Vehicle
I-DEMS	Intelligence Dynamic Energy Management System
PEV	Plug-in Electric Vehicle
MILP	Mixed Integer Linear Programming
NPV	Net Present Value
OBESS	Optimal Battery Energy Storage System
DSO	Distribution System Operator
RLA	Reinforcement Learning Alghorithm
AA	Affine Arithmetic method
CERTS	Consortium for Electric Reliability Technology Solutions
SC	Super Capacitor
PCC	Point of Common Connection
NFL	Not Free Launch
SSA	Salp Swarm Alghorithm
$P_i(t)$	amount of generation
$\pi_i(t)$	generation cost
$I_i(t)$, $I_{BUY}(t)$, and $I_{Sell}(t)$	binary variables
$SU_i(t)$	specifies the cost of starting
$P_{Grid-Buy}$ and $P_{Grid-Sell}$	amount of power received or sent
$P_{Demand}(t)$	power demand
x_j^1	leader in the *jth* dimension
F_j	the location of the food source in the *jth* dimension
ub_j, lb_j	Upper and lower limit of the *jth* dimension
c_1, c_2, and c_3	random numbers
i	iteration
L	maximum number of iterations
v_o	initial speed
$f(w)$	Weibull probability distribution function
r	related to the shape
q	scale parameter
w_{mean}	mean
σ^2	variance
$\Gamma(x)$	gamma function
w	wind speed
ρ	air concentration
R	rotor radius
C_p	coefficient
w_1, w_r, and $w_{cut\ out}$	cut-in, nominal, and cut-out speeds
k_1 and k_2	constant coefficients
P_{nom}	nominal power of the turbine
si	amount of radiation
η^{PV}	panel efficiency
η^{PV} and A^{PV}	panel efficiency and area
μ_{si} and σ_{si}^2	mean and the variance of the radiation
$L_{d_{mean}}$ and $\sigma_{L_d}^2$	mean and variance of the consumer demand
$\eta_{disCharge}$ and η_{Charge}	battery discharge and charge efficiency
$I_{disCharge}$ and I_{Charge}	binary variables that cannot have a value of one at the same time
π_ (Grid-Buy) (t) and π_ (Grid-Sell) (t)	the prices of power units exchanged between the MG and the main grid

Strategy (OS). In Ref. [3], real-time energy management is carried out for a micro-grid with a renewable generation system, an energy storage system, and an integrated load., aiming to minimize the total cost of energy. To solve the problem in real time, a new offline optimization approach is used in order to derive the online algorithm. In Ref. [4], an algorithm-based method is proposed to determine the size of Energy Storage Systems (ESS) in microgrids. The main goal of this method is to determine the energy capacity and power of the storage system, which minimizes the operating costs of the microgrid. The work by Ref. [5] presents the 24-h power distribution optimization problem for a microgrid with Distributed Energy Resources (DERs), including variable loads with direct control. In Ref. [6], the technical background of microgrid scheduling optimization methods is reviewed, and guidelines are defined for innovative scheduling methods, focusing on economic feasibility. In Ref. [7], a robust optimization-based approach for optimal microgrid management is presented with regard to wind energy uncertainty. In Ref. [8], a new multi-objective energy management method for microgrids is presented, which includes RESs, diesel generators, battery storage, and different loads. In Ref. [9], a new battery performance cost is presented, considering the battery and a generator with equivalent fuel consumption to charge it, as well as proposing a unit contribution problem. The authors of [10] a two-stage framework is presented for the economic operation of a microgrid-like Electric Vehicle (EV) with renewable energy generation (rooftop with photovoltaic panels). In Ref. [11], an energy management system for a smart microgrid is presented. The work by Ref. [12] proposes a multi-objective load distribution with the presence of a Plug-in Electric Vehicle (PEV) as storage unit. Energy storage planning is designed as a Mixed Integer Linear Programming (MILP) model according to PEV requirements, minimizing three different objectives and analyzing three different criteria. In Ref. [13], a design approach is evaluated with the aim of integrating the energy management and sizing of a small microgrid in the presence of storage systems. The authors of [14] consider the principles of energy management for supply/demand coordination, showing that this concept is effective in managing energy demand response and dynamic data flow in the field of microgrid energy systems. A detailed description of the progress in demand-side management, demand response programs, DG, technical issues in process, and its key benefits in microgrids is provided by Ref. [15]. In Ref. [16], the Net Present Value (NPV) is considered to minimize the total expected costs over a multi-year period, given the optimal performance of an Optimal Battery Energy Storage System (OBESS), as well as according to a new matrix that represents the reduction of BESS energy capacity. The work by Ref. [17] describes the two-level formulation of a planning problem concerning microgrid and stored energy capacity in the vicinity of the Distribution System Operator (DSO). In Ref. [18], a stochastic programming model is proposed to optimize the performance of a smart microgrid in the short term, aiming to reduce operating costs and emissions with renewable resources. The authors of [19] present an approach for optimal microgrid planning, which includes various distributed resources such as databases and DG units. In Ref. [20], the energy management of home smart AC/DC hybrid micro-grids with the ability to change the structure is considered with respect to combined thermal and electrical loads (CHP) such as the charging/discharging behavior of electric vehicles. The work by Ref. [21] proposes a powerful mathematical formulation for the energy management systems of islanded microgrids while including renewable energy sources, energy storage, and interruptible loads. In Ref. [22], production units and microgrid subscribers are modeled as independent agents who are able to make local decisions for their maximum efficiency in a multi-agent environment. The authors of [23] study a network-connected microgrid with a BESS, PV generation, and different loads. Finally, in

Ref. [24], a mathematical formulation for islanded microgrid energy management systems is presented, which considers the uncertainties of the consumption load and the power of renewable energy sources by means of the Affine Arithmetic (AA) method. In Ref. [25], Application of the arithmetic optimization algorithm to solve the optimal power flow problem in direct current networks, In Ref. [26] An innovative synthesis of optimization techniques (FDIRE-GSK) for generation electrical renewable energy from natural resources and in Refs. [27,28] The effectiveness of the wind barrier in mitigating soiling of a ground-mounted photovoltaic panel at different angles and particle injection heights, Parametric optimization of novel solar chimney power plant using response surface methodology studied.

1.2. Contribution and paper organization

This research considers distribution network subsystems consisting of DERs, ESSs, and connected loads that are operated via a single control system that is either connected or isolated from the grid. The ever-increasing need to effectively meet the energy demand has aroused much interest in the concept of microgrids. MGs can effectively manage and coordinate distributed load generation resources, as well as support a high penetration of RESs.

This paper is divided into six sections.

- The suggested methodology provides optimal operation for the microgrid considering the uncertainty in generation, load, and price.
- The proposed methodology takes into account the generation cost and emission cost of different resources.
- The introduced technique is applied to grid-connected and grid-islanded microgrids.
- The optimization problem is a mixed integer, which is handled efficiently using the proposed slap swarm optimization algorithm.

In section 2, microgrids including (AC microgrids, DC microgrids and hybrid microgrids) are presented. In section 3. Optimization problem is discussed. In section 4 of the method, the investigation of the equations of the sources and the studied system will be investigated. Section 5. The simulation results are fully discussed. Finally, some conclusions will be drawn from the article.

2. Microgrids

The concept of *microgrid* was coined by the CERTS Institute [29]. A MG is defined as a local entity consisting of DERs and controllable thermal and electrical loads. To receive power, these loads are connected to the upstream grid, which may use solar panels (PV), wind power plants, fuel cells, diesel generators, and micro-turbines with a storage device (such as a battery or a Super-Capacitor (SC) [30]. From an operation perspective, MGs can be regarded as a controlled cell or battery. From a consumer (customer) perspective, a MG is designed to meet reliability conditions, reduce feeder losses, improve efficiency, and minimize voltage drops and guarantee a continuous power supply [31]. In general, the types of MGs in power systems can be divided into two parts, AC and DC, which is discussed below.

2.1. AC microgrids

In an AC microgrid, distributed generators and energy storage systems are connected to the AC bus through power electronic devices. By using the on/off control at the Point of Common Connection (PCC), the MG can be switched to two modes: grid-connected or islanded. Fig. 1 shows an AC microgrid [32].

2.2. DC microgrids

AC and DC loads at different voltage levels can be fed with a DC microgrid through power electronic converters. Changes in the power generation of distributed sources and the power consumption of loads can also be adjusted by using ESSs connected to the DC bus. In a DC microgrid, DG sources are connected to the DC bus through a voltage converter. This structure is more economical when there are many DC power sources and loads in the system. Fig. 2 shows the structure of a DC microgrid [32,33].

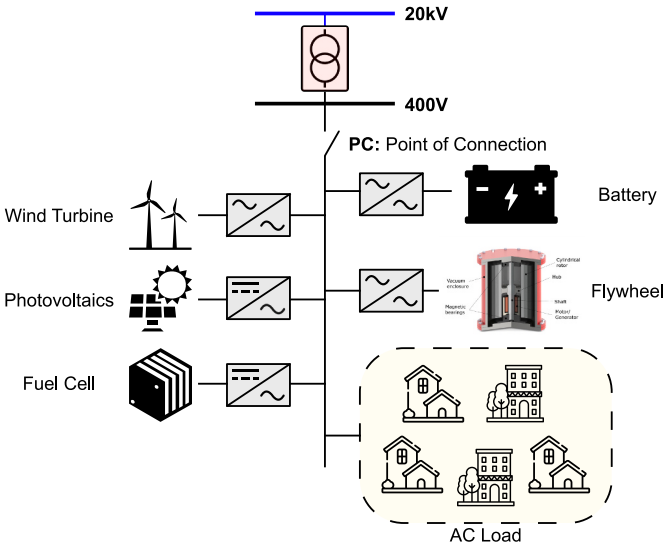

Fig. 1. AC micro-grid with the ability to connect to the network or operate in islanded mode.

2.3. AC-DC hybrid microgrids

A hybrid AC-DC microgrid consists of DC and AC buses and feeds both DC and AC loads. Hybrid MGs can be considered as an AC microgrid where the DC grid is connected to the AC bus through an inverter and acts as a power source. A hybrid AC-DC microgrid has the characteristics of both AC and DC microgrids and can better feed different loads. The structure of this type network is shown in Fig. 3 [32].

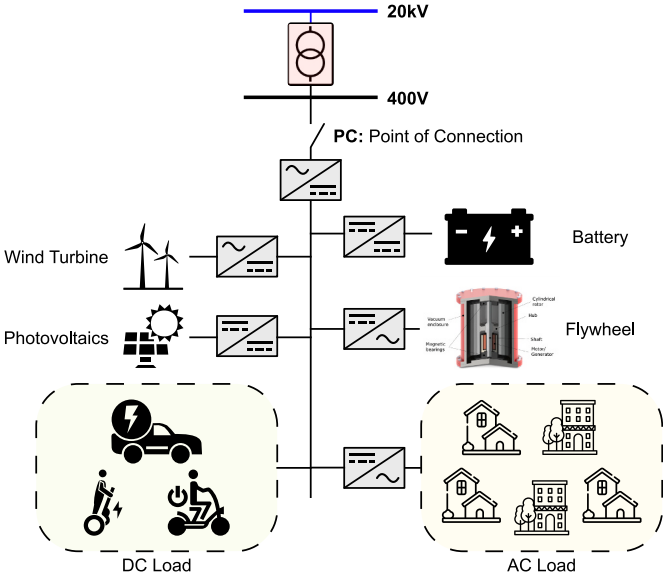

Fig. 2. DC microgrid with the ability to connect to the network or operate in islanded mode.

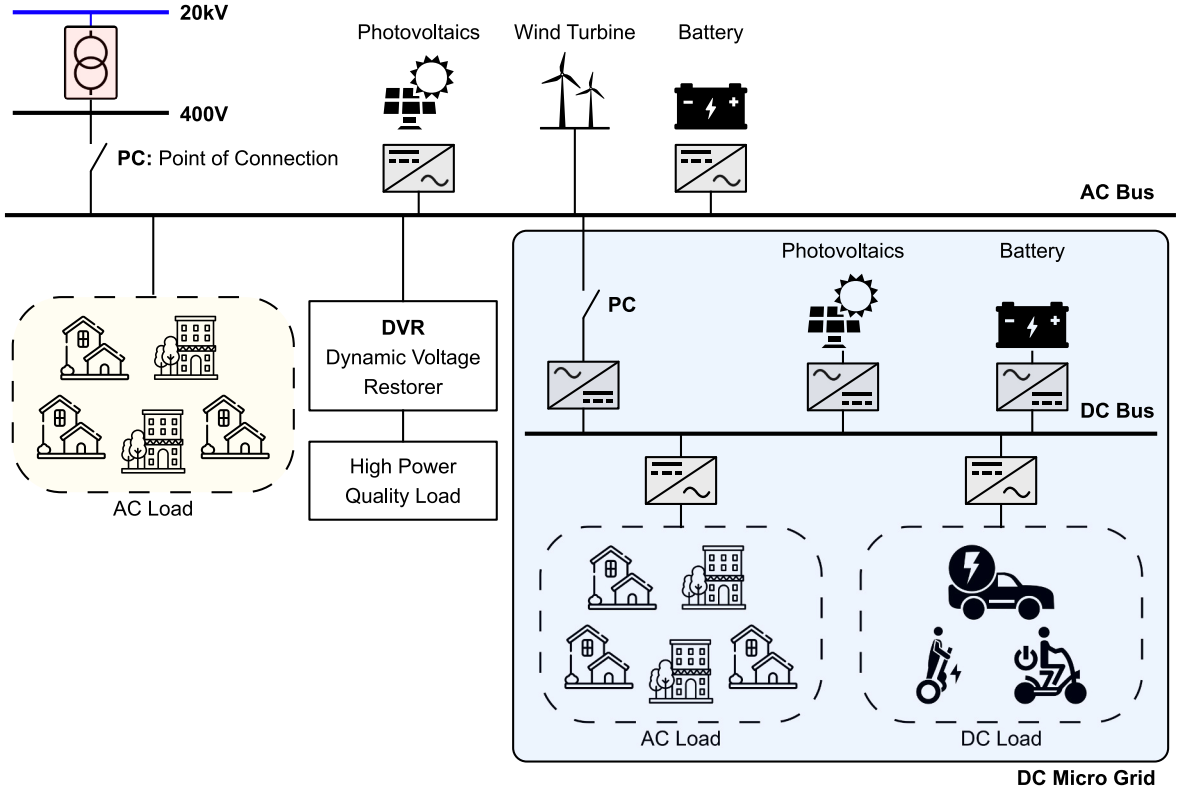

Fig. 3. AC-DC micro-grid with the ability to connect to the network or operate in islanded mode.

3. Optimization problem

Traditional methods for solving optimization problems, which are known as exact optimization methods, have a high computational complexity. Collective intelligence algorithms based on the collective behavior of agents have partially solved this problem, and the results obtained by these algorithms are very close to optimal solutions [34,35]. The standard form of an optimization problem (continuous) is expressed in Eq. (1).

$$\min_{x} f(x) g_i(x) \leq 0 h_i(x) = 0 \tag{1}$$

Where $f(x) : \mathbb{R}^n \rightarrow \mathbb{R}$ is the objective function that tends to be minimized on the vector variable x, $g_i(x) \leq 0 \quad i = 1, 2, \ldots, m$ are the constraints of the inequalities and, $h_i(x) = 0, i = 1, 2, \ldots, n$ are the equality constraints.

The main characteristic of this optimization problem (1) is that it looks for a vector x proportional to the dimensions of the problem, with two important properties. First, it must satisfy both sets of constraints, *i.e.*, $g_i(x) \leq 0 \quad i = 1, 2, \ldots, m$ and $h_i(x) = 0, i = 1, 2, \ldots, n$. Secondly, the value of the function f(x) for the desired x must be at its lowest value. Some problems deal with the maximization of an objective function, which can be replaced by a minimization problem, as shown in Eq. (2).

$$max\, f(x) = \min(-f(x)) \tag{2}$$

In solving the above optimization problem, the constraints of the problem are prioritized. In other words, (i) the constraints determine the range of the vector x in the n-dimensional space, and (ii) the value of x is selected from this range, for which the function f(x) is at the lowest value. In some cases, when the two sets of inequality and equality constraints do not have a common point, the problem is dubbed *impossible*, and it cannot be solved under the desired conditions. To solve the optimization problem in the form of (1), many metaheuristic methods have been introduced, in addition to the mathematical methods described in the previous subsection.

4. Methodology

This section describes the role of the SALP Swarm Algorithm (SSA) in the energy management and performance of microgrids.

4.1. SALP Swarm Algorithm (SSA)

Salps belong to the family Salpidae, and they are creatures with a transparent and tubular body (Fig. 4a) [36,37]. Their body texture is very similar to that of jellyfish, and they move much like them, pumping water through their bodies to provide forward thrust. The SSA imitates their social and chain-like behavior, as their movement involves rapid and coordinated changes for chasing food.

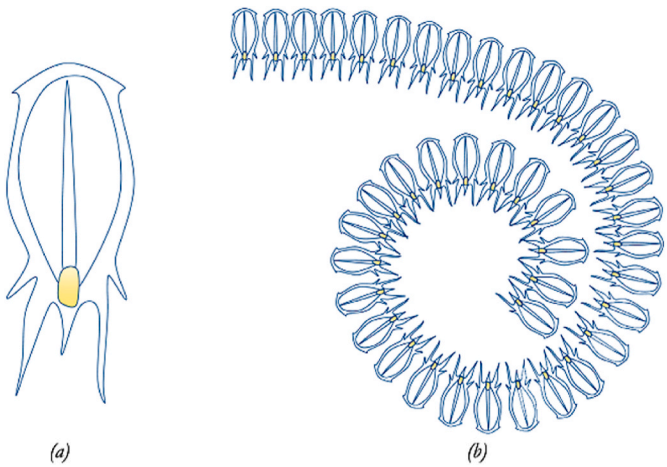

Fig. 4. (a) Single salp, (b) salp chain [37].

4.1.1. Proposed mathematical model

Similar to other collective methods, the position of salps is defined in an n-dimensional search space, where n is the number of variables of a given problem. Thus, the position of all salps is stored in a two-dimensional matrix (x). It is also assumed that there is a food source (F) in the search space, which constitutes a collective purpose. To update the position of the first salp (leader), Eq. (3) is used.

$$x_j^i = \begin{cases} F_j + C_1\left(\left(ub_j - lb_j\right)C_2 + lb_j\right).C_3 \geq o \\ F_j - C_1\left(\left(ub_j - lb_j\right)C_2 + lb_j\right).C_3 < o \end{cases} \tag{3}$$

Where x_j^1 represents the position of the leader in the *jth* dimension; F_j is the location of the food source in the *jth* dimension; ub_j represents the lower limit of the *jth* dimension; and c_1, c_2, and c_3 are random numbers. Eq. (3) shows that the leader only updates its position relative to the food source. The coefficient c_1 is the most important parameter in the SSA algorithm because it balances exploration and exploitation, which is defined by Eq. (4).

$$c_1 = 2e^{-\left(\frac{*i}{l}\right)^2} \tag{4}$$

Where *i* is the current iteration and L is the maximum number of iterations. Parameters c_2 and c_3 are random numbers generated uniformly in the interval [0, 1]. These indicate whether the next position in the *jth* dimension should be towards positive infinity or negative infinity, and the also specify the step size. To update the salp followers' position, Eq. (5) are used (Newton's law of motion).

$$x_j^i = \frac{1}{2}at^2 + v_o t \tag{5}$$

Here, $i \geq 2$ indicates the position of the *ith* follower in the *jth* dimension; t is the time; v_o is the initial speed; and $a = \frac{v_{final}}{v_o}$ (Eq. (6)).

$$v_o = \frac{x - x_o}{t} \tag{6}$$

Because *time* and *iterations* are the same thing in the context of optimization, the difference between iterations is equal to 1. Thus, assuming $v_o = 0$, this equation can be written by Eq. (6).

$$x_j^i = \frac{1}{2}\left(x_j^i + x_j^{i-1}\right) \tag{7}$$

Where $i \geq 2$, and x_j^i indicates the position of the *ith* follower in the *jth* dimension. The SSA is able to move salps to the food source and update them in each iteration. However, this algorithm is unable to solve multi-objective functions for two reasons: (i) the SSA cannot store multiple solutions for a multi-objective function, and (ii) it updates the food source with the best solution in each iteration, but there is no single best solution for multi-objective functions. The higher the number of responses neighboring a solution (*i.e.*, the larger the rank number), the more likely it is to be removed from the pool. The pseudo-code of the SSA is shown in Algorithm 1 [37].

Algorithm 1
SSA pseudo-code [37].

Initialize and create the initial population of salps according to the upper and lower bounds of *lb*, *ub* **while** (until the stopping condition is met)
Calculate the objective function for each agent
Select the best search factor

(*continued on next column*)

Algorithm 1 (*continued*)

Update *c1* using Eq. (4) **for** loop for each salp
if (*i*==*1*)
Update the position of the leader according to Equation (3)
Otherwise
Update follower position using Eq. (5) end
end
Check the position of salps in the range of *lb*, *ub* end

4.2. Modeling wind system uncertainty

The output power of the wind turbine depends on parameters such as wind accessibility, the wind turbine power curve, wind speed, and the shape and size of the turbine. Therefore, since the wind speed is random, the Weibull probability distribution function is suitable for modeling it at any given moment. The Weibull can model wind speed changes caused by different weather changes. This function is presented in Eq. (8) [38].

$$f(w) = \frac{r}{q}\left(\frac{w}{q}\right)^{r-1} exp\left(-\left(\frac{w}{q}\right)^r\right) \tag{8}$$

In the above equation, f(w) is the Weibull probability distribution function for the wind speed, the parameter r is related to the shape, and q represents the scale parameter. In addition, the relationship between the parameters of the Weibull function and the mean and the variance of the distribution function (Eq. (9) and Eq. (10)).

$$w_{mean} = q\Gamma\left(1 + \frac{1}{r}\right) \tag{9}$$

$$\sigma^2 = q^2\left(\Gamma\left(1 + \frac{2}{r}\right) - \left(\Gamma\left(1 + \frac{1}{r}\right)\right)^2\right) \tag{10}$$

Where, w_{mean}, σ^2, and $\Gamma(x)$ are the mean, the variance of the probability function, and the *gamma* function, respectively. The mean and variance of the parameters r and q are calculated according to Eq. (11) and Eq. (12) [38].

$$r = \left(\frac{\sigma}{w_{mean}}\right)^{-1/086} \tag{11}$$

$$q = \frac{w_{mean}}{\Gamma\left(1 + \frac{1}{r}\right)} \tag{12}$$

In this way, the wind turbine production power can be obtained, which depends on the wind speed (w), air concentration (ρ), rotor radius (R), and performance coefficient (C_p), as shown in Eq. (13).

$$S_{WT}(w) = \frac{1}{2}\rho\pi R^2 C_p(\lambda)w^3 \tag{13}$$

Finally, the amount of power produced by the wind turbine can be linearly estimated according to Eq. (14).

$$\begin{cases} o & .0 \leq w \leq w_1 \quad .w \geq w_{cut\ out} \\ P_{nom}(k_1 + k_2 w) & .w_1 \leq w \leq w_r \\ P_{nom} & .w_r \leq w \leq w_{cut}\ out \end{cases} \tag{14}$$

Where w_1, w_r, and $w_{cut\ out}$ are the low cut-in, nominal, and cut-out speeds. Moreover, k_1 and k_2 are two constant coefficients related to the wind turbine, and P_{nom} is the nominal power of the turbine.

4.3. Modeling PV system uncertainty

The amount of power produced by a solar panel depends on the amount of radiation it receives. In this vein, the amount of power, which is dependent on the panel surface, the efficiency percentage, and the amount of radiation, can be determined through Eq. (15).

$$S_{PV}(si) = \eta^{PV} A^{PV} si \tag{15}$$

Where *si* is the amount of radiation in kilowatts per square meter; and η^{PV} and A^{PV} are the panel efficiency and area, respectively. As it is known, the amount of radiation received by the panel is uncertain, so the probability distribution function for the amount of radiation is defined in a different way, as shown in Eq. (16) [38].

$$f_b(si) = \begin{cases} \frac{\Gamma(\alpha+\beta)}{\Gamma(\alpha)\Gamma(\beta)}\, si^{(\alpha+1)}(1-si)^{(\beta-1)} & for\ 0 \le si \le 1\ ,\ \alpha \ge 0\ ,\ \beta \ge 0 \\ \cdot \quad o \cdot w. \end{cases} \tag{16}$$

Furthermore, the two parameters α and β in the above relationship are determined according to Eq. (17) and Eq. (18).

$$\beta = (1-\mu_{si})\left(\frac{\mu_{si}(1+\mu_{si})}{\sigma_{si}^2} - 1\right) \tag{17}$$

$$\alpha = \mu_{si} * \frac{\beta}{1-\mu_{si}} \tag{18}$$

In these two relationships, μ_{si} and σ_{si}^2 are the mean and the variance of the radiation, respectively.

4.4. Modeling consumption load uncertainty

In this section, three types of consumers are considered for the network: residential, commercial, and industrial. Their consumption, like the amount of radiation or wind speed, is always somewhat uncertain [39,40], which must be considered in the model. Eq. (19) shows the load probability distribution function.

$$f_{load}(L_d) = \frac{1}{\sqrt{2\pi\sigma_{L_d}^2}} \exp\left(-\frac{(L_d - L_{d_{mean}})^2}{2\sigma_{L_d}^2}\right) \tag{19}$$

Where $L_{d_{mean}}$ and $\sigma_{L_d}^2$ are the mean and variance of the consumer demand, respectively.

4.5. Modeling the uncertainty of electricity pricing

Eq. (20) shows the probability density distribution function of electricity pricing, where $price_{mean}$ is the average price and σ_{price}^2 represents its variance. Usually, each MG connected to the upstream grid buys power from the main grid when there is a shortage, and it sells it to the grid when there is excess power generation. In this research, it is assumed that the buying and selling prices are equal, and it is also assumed that the price is uncertain, which is calculated according to Eq. (20).

$$f_{MarketPrice}(price) = \frac{1}{\sqrt{2\pi\sigma_{price}^2}} \exp\left(-\frac{(L_d - price_{mean})^2}{2\sigma_{price}^2}\right) \tag{20}$$

4.6. Operating costs function

This function is shown in Eq. (21). Certain operating costs include fixed start-up costs, the costs of turning on DG sources, and the costs of exchanging power with the upstream network. Eq. (22) expresses the $CC(t)$ term of the above cost function.

$$F_1(x) = \sum_{t=1}^{24} (CC(t)) \tag{21}$$

$$CC(t) = \sum_{i=1}^{N_{DG}} (P_i(t)\pi_i(t)I_i(t) + SU_i(t)|I_i(t) - I_i(t-1)|) + I_{BUY}(t)P_{Grid-Buy}(t)\pi_{Grid-Buy}(t) - I_{Sell}(t)P_{Grid-Sell}(t)\pi_{Grid-Sell}(t) \tag{22}$$

In this relation, $P_i(t)$ is the amount of generation and $\pi_i(t)$ is the generation cost of the *i*th unit at time t. $I_i(t)$, $I_{BUY}(t)$, and $I_{Sell}(t)$ are binary variables that indicate the presence or absence of the corresponding term at the *tth* moment in the objective function. $SU_i(t)$ also specifies the cost of starting up or shutting down the *i*th unit at time t. Also, $P_{Grid-Buy}$ and $P_{Grid-Sell}$ show the amount of power received or sent. One of these two values can be non-zero at any time. π_ (Grid-Buy) (t) and π_ (Grid-Sell) (t) are the prices of power units exchanged between the MG and the main grid. As previously mentioned, these two parameters are considered equal in this research.

4.7. Emission cost function

The pollution emission function includes the amount of pollution caused by DG units and that caused by the network in energy purchasing. The considered pollutants include SO_2, CO_2, and NOx. The mathematical model of the pollution emission function is expressed in Eq. (23).

$$F_2(x) = \sum_{t=1}^{24} (EMI_{DG}(t) + EMI_{Grid}(t)) \tag{23}$$

The average pollution caused by non-renewable distributed generation units can be calculated according to Eq. (24). Where $E_{CO_2}(i)$, $E_{SO_2}(i)$, and $E_{NO_x}(i)$ are the emitted amounts of the above-mentioned gases. In the same way, the pollution caused by the network when buying energy is determined via Eq. (25).

$$EMI_{DG}(t) = \sum_{i=1}^{24} (E_{CO_2}(i) + E_{SO_2}(i) + E_{NO_x}(i))P_i(t) \tag{24}$$

$$EMI_{Grid}(t) = \sum_{t=1}^{24} \left(E_{CO_2}^{Grid} + E_{SO_2}^{Grid} + E_{NO_x}^{Grid}\right) P_{Grid}(t) \tag{25}$$

4.8. Limitations of the planning problem

MG planning involves limitations that must be observed while determining the grid's parameters. The following subsections discuss the constraints to be considered for generation planning.

4.9. Power equality constraint

The total power produced by DG sources and that purchased from the network in each interval and scenario must be equal to the total demand load (Eq. (26)). In this equation, $P_{Demand}(t)$ is the power demand at any time *t*.

$$\sum_{i=1}^{N_{DG}} P_{DG}(t) + P_{Grid}(t) = \sum_{l=1}^{N_s} P_{Demand}(t) \tag{26}$$

4.10. Generation power limitation

The maximum and minimum power produced by each unit is limited according to Eq. (27).

$$P_{DG,i}^{min} \le P_{DG,i}(t) \le P_{DG,i}^{max} \tag{27}$$

4.11. Battery limitations

Regarding the battery, there are three basic limitations that must be considered during planning (Eq. (28), Eq. (29) and Eq. (30)) [41].

$$W_{ess}(t) = W_{ess}(t-1) - \frac{1}{\eta_{disCharge}} I_{disCharge}(t) P_{disCharge} + \eta_{Charge} I_{Charge}(t) P_{Charge} \tag{28}$$

W_{ess} shows the amount of energy stored in the battery, and $\eta_{disCharge}$ and η_{Charge} represent the battery discharge and charge efficiency, respectively. In this regard, $I_{disCharge}$ and I_{Charge} are binary variables that cannot have a value of one at the same time (Eq. (29)).

$$I_{Charge} + I_{disCharge} \leq 1 \tag{29}$$

Eq. (30) shows the battery capacity, which can change depending on the amount of energy charged and discharged per hour.

$$W_{ess}^{min} \leq W_{ess}(t) \leq W_{ess}^{max} \quad P_{charge}(t) \leq P_{charge}^{max} P_{discharge}(t) \leq P_{discharge}^{max} \tag{30}$$

4.12. Studied system

In this section, a sample MG is examined, and the proposed algorithm is simulated on it. This MG comprises a solar cell generator with an area of 10 m^2 and an efficiency of 18.6%. A 25 kW SOLAREX MSX solar cell consisting of 10 2.5-kW solar panels has been selected. The amount of radiation received by the solar cell is shown in Fig. 5. Of course, as stated before, the amount of solar radiation is always uncertain. The probability density function described above is also given in Fig. 5, *i.e.*, the radiation curve and its uncertainty. It should be noted that the power factor of the solar panel is assumed to be 1.

The wind speed for a 24-h cycle is considered (Fig. 6), in addition to its uncertainty.

Another parameter considered for the sample MG is the load consumed per hour. As mentioned earlier, residential, commercial, and industrial loads are considered, which are also subject to uncertainty. The nominal value is given in Fig. 7. In addition, Fig. 8 shows the nominal total with the uncertainty of the three consumer categories per hour. The total load considered for a 24-h period is 4034 kW.

Here are two points to consider regarding the price of power exchange between the main grid and the MG.

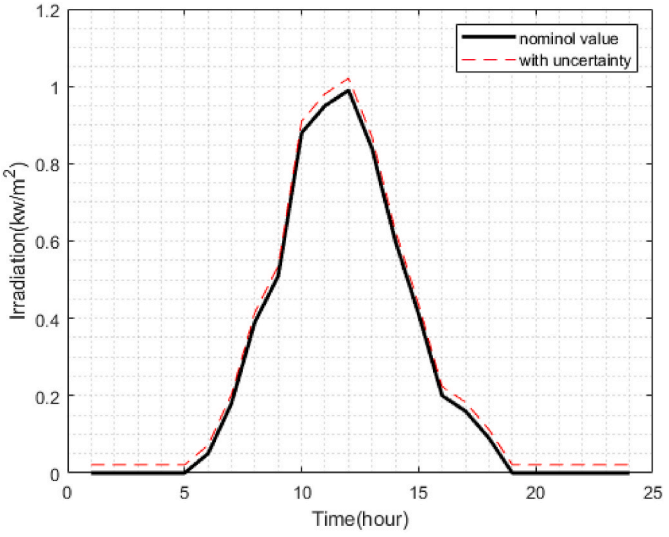

Fig. 5. Nominal amount of radiation received by the solar cell along with the uncertainty for one day and one night.

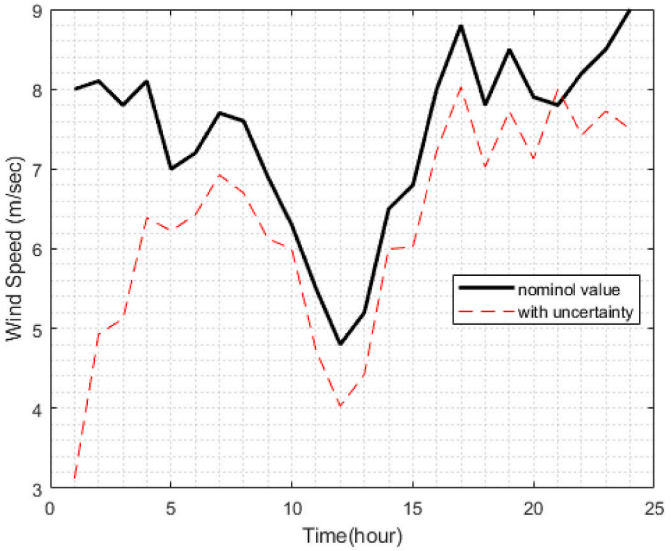

Fig. 6. Nominal wind speed and uncertainty for during one day and one night.

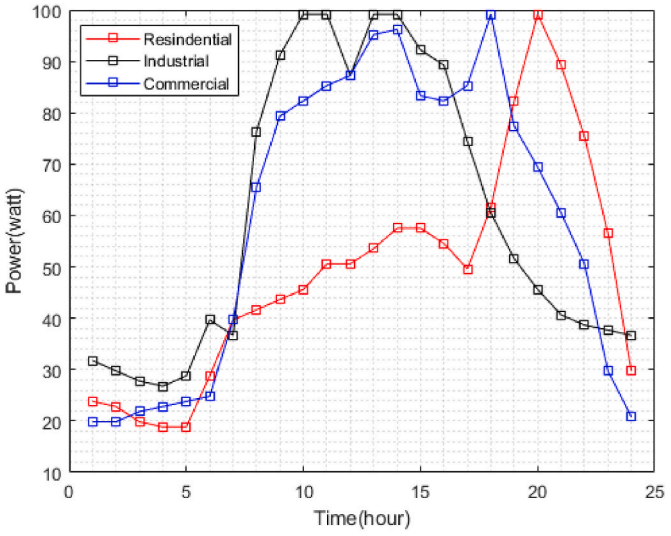

Fig. 7. Nominal power characteristics of three residential, industrial, and commercial loads for a day of operation.

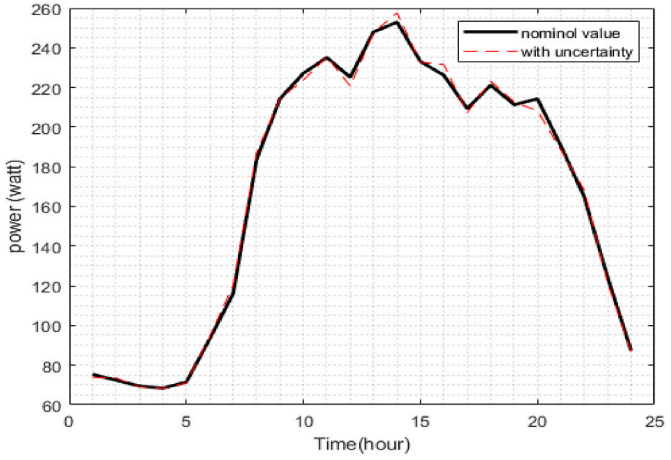

Fig. 8. Nominal power consumer demand (load) and uncertainty for a day and a night.

Table 1
MG parameters [42].

	Unit type	Bid (Euro/kWh)	Start-up/shut-down cost (Euro)	CO_2 (kg/MWh)	SO_2 (kg/MWh)	NO_x (kg/MWh)	Low power limit (kW)	High power limit (kW)
1	Diesel generators	0.586	0.15	890	0.0054	0.23	30	300
2	Microturbines	0.457	0.96	720	0.0036	1.0	6	30
3	Fuel cells	0.294	1.65	460	0.003	0.0057	3	30
4	Photovoltaic panels	2.584	0	0	0	0	0	25
5	Wind turbines	1.073	0	0	0	0	0	15
6	Batteries	0.38	0	10	0.0002	0.0001	−30	30
7	Network	0	0	950	0.5	1.2	−30	30

1) The price of power exchange is not the same for all 24 h. At some points, due to time sensitivity, the price increases.
2) The nominal value of the price with uncertainty (Fig. 9) is under the influence of the market.

Other elements in the MG, namely the micro turbine, diesel generator, and battery, also include parameters that are not considered uncertain. Table 1 shows the cost of power generation by MG component, harmful gas emissions, and the power limit of each component.

As shown in the table, battery charging and discharging are limited to +30 and −30 kW, respectively. The value of battery charge and discharge efficiency is assumed to be 0.94. Simulations were carried out in several stages, as explained in the introduction of this paper.

5. Results

All simulations were run in MATLAB. The parameters of the implemented algorithm, apart from its number of variables, were completely fixed, which is explained below. The maximum iterations were set as 1000. The initial population was 100.

Moreover, the number of variables for when the MG is isolated from the main grid is related to photovoltaic, wind turbine, diesel generator, fuel cell, and microturbine generation, as well as to the charge and discharge rate of the battery.

5.1. Operation of an islanded microgrid with parameter certainty

In the first case, it is assumed that all MG parameters are certain, including photovoltaic and wind turbine generation, as well as the amount of power demanded by consumers, and the microgrid does not exchange any power. The parameters of the optimization algorithm were chosen according to the previously presented information, and the number of variables was set to 6. The results for the objective function value are given in Fig. 10.

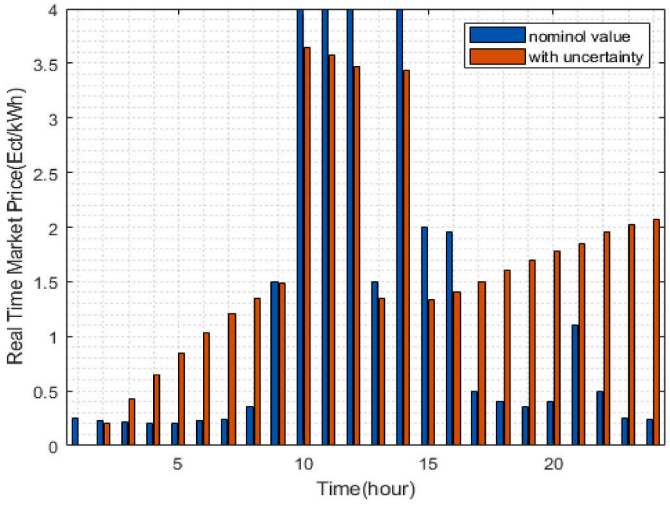

Fig. 9. Real-time Market Price Nominal value and uncertainty for the exchange of power between the MG and the main grid during a day and a night of operation.

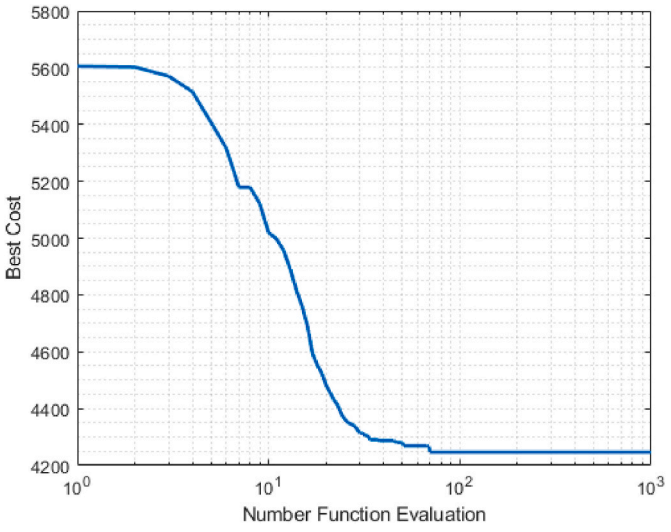

Fig. 10. Results for the objective function value.

According to Fig. 10, the final and optimal value for the objective function is 4200.42 units. This, as previously stated, includes two separate terms: the cost of operation and the cost of pollutant production, which amount to 816.2 and 1170.54 units of the total value. Therefore, production equal to demand will be 2213.68. Fig. 11 is a diagram of the production power values of the resources.

5.2. Operation of an islanded microgrid with parameter uncertainty

In this case, it is assumed that the parameters of load and photovoltaic, wind turbine generation are uncertain. The other parameters are treated as in case 1. Note that, in this mode, the MG operates independently and feeds its own loads. This objective function also includes terms: operating and production costs, the costs implied by the production of polluting gases, and the penalty for the inequality of production and demand. The total optimal cost obtained from the algorithm is 4240.63 units, out of which 803.24 and 1023.56 are related to the first two costs, and the rest is related to the third term. The cost increase compared to the first case is due to the uncertainty in the power generation of wind turbines and photovoltaic panels. The results of this section are shown in Fig. 12.

5.3. Operation of a grid-connected microgrid with parameter certainty

The third case is the same as the first state, with the difference that the MG has the possibility of exchanging power with the main grid. In

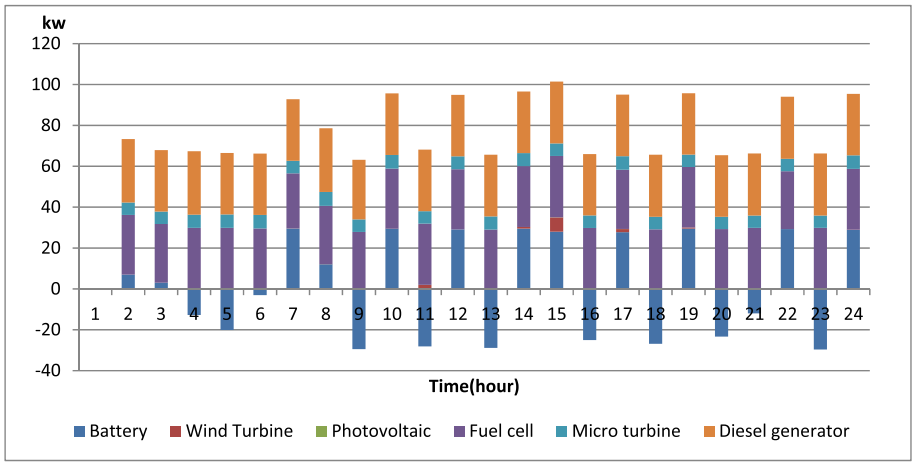

Fig. 11. Power generation diagram for case 1.

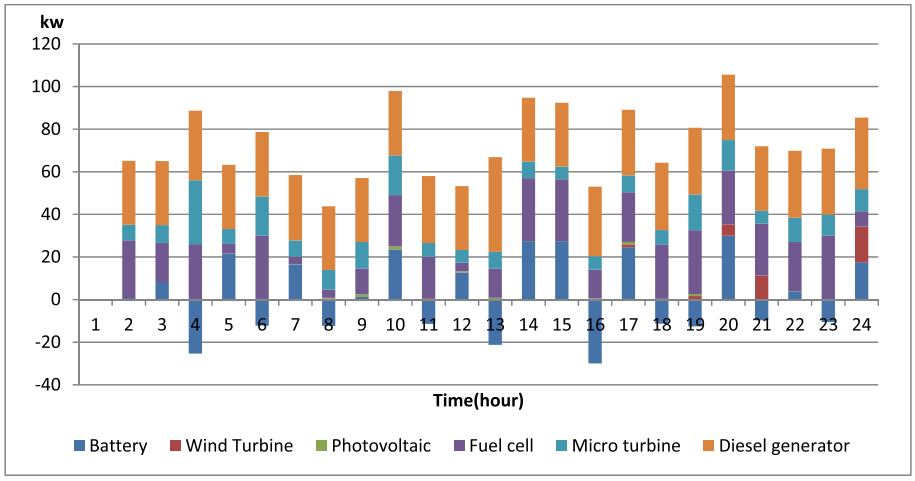

Fig. 12. Power generation diagram for case 2.

this way, when there is excess generation, it can sell it to the network, and it can receive power if there is a shortage. The price of power exchange between the main grid and the MG has already been stated, and the remaining parameters are set as in case 1.

Three different terms have been considered for the objective function of this algorithm. The final and optimal value of the total objective function is 4157.63 units, with 803.24 and 1023.56 being the cost of operation and the production of pollutants, respectively. The main difference lies in the fact that more iterations were required than in the two previous scenarios. In the two previous cases, there was a decreasing trend until about 100 iterations, and then the objective function value was almost constant. The results obtained in this case are explained by the higher complexity of the problem, as it adds a variable. According to the results, in the hours when the electricity market price is high, the MG sends power to the main grid, thus increasing microturbine generation. This also means less charging of the battery. Moreover, the connection to

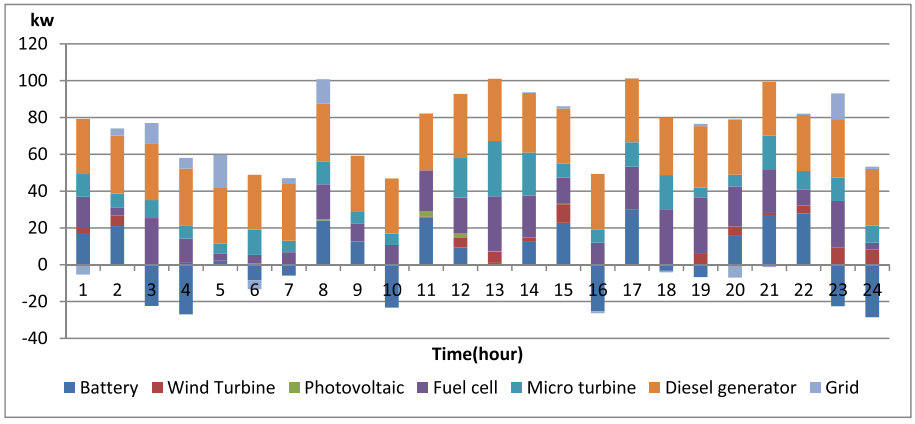

Fig. 13. Power generation diagram for case 3.

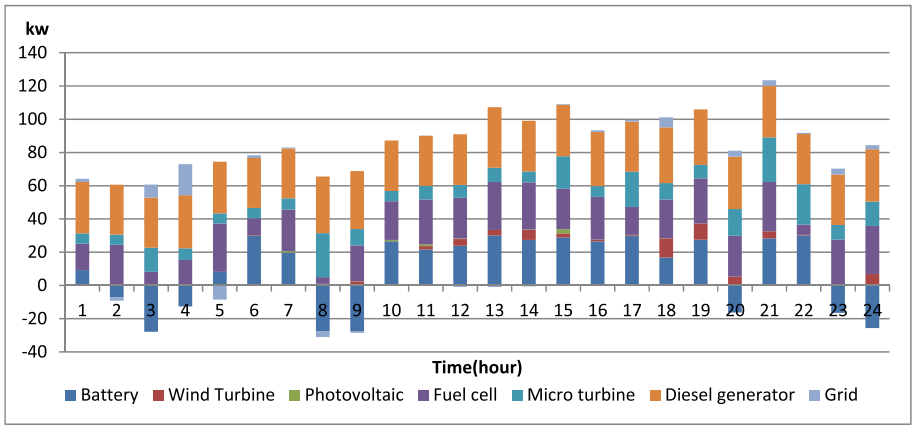

Fig. 14. Power generation diagram for case 4.

the network reduces the analyzed costs, which results in the reduction of the overall objective function and power generation diagram case 3 show in Fig. 13.

5.4. Operation of a grid-connected microgrid with parameter uncertainty

In this scenario, the MG is connected to the main grid for 24 h, and the parameters are uncertain. These parameters include the PV and wind turbine generation, as well as the load and the price of power exchange. The optimal value of the objective function for this scenario is 4121.52 units, out of which 810.34 and 1117.6 are related to operation costs and pollution. Fig. 14 shows the power generation.

5.5. The operation of microgrid with uncertainty considering the cost of production and operation

This scenario is similar to the previous one, with the difference that the objective function includes only the cost of production and operation. Table 2 shows the power generation for case 5 and Table 3 shows the power generation for case 6.

5.6. The operation of the microgrid with uncertainty considering the amount of pollution

This scenario is similar to case 4, but the objective function only includes the cost of pollution. By comparing cases 5 and 6, it can be seen that, if the goal is to reduce the costs of production and operation of the network, the production rate of the photovoltaic system will decrease, and solar energy will have higher costs. If the goal is to reduce emissions, the production rate of the diesel generator unit will decrease, power generation and storage planning in the microgrid for case 6 in Table (3).

6. Conclusion

The article introduced a metaheuristics technique, Salp Swarm algorithm, for the optimal operation of a microgrid during different scenarios, such as grid-connected and grid-islanded operation modes. Moreover, the proposed technique minimized the generation cost and the emission cost considering the uncertainties of generation, load, and energy price. The introduced optimization algorithm, which is an adaptation of the behavior of salps in nature, proved its efficiency in handling the optimization problem, which has continuous variables

Table 2
The results of power generation and storage planning in the microgrid for case 5.

Hour	Grid (kW)	Battery (kW)	Wind Turbine (kW)	Photovoltaic (kW)	Fuel cell (kW)	Micro turbine (kW)	Diesel generator (kW)
1	12.46	1.01	0	0	11.76	8.02	31.34
2	.99	2.18	0	0	3.96	6.20	58.27
3	−.28	−4.37	.01	0	17.02	12.70	43.35
4	.30	5.39	.27	0	10.27	6.96	43.61
5	3.81	2.24	2.04	0	7.61	7.22	48.09
6	2.87	4.27	.07	0	3.90	9.90	71.61
7	28.28	−.48	.07	.08	3.73	9.54	72.70
8	17.99	−6.90	.48	.82	3.63	15.74	146.30
9	26.62	−1.84	1.51	.31	13.24	6.26	164.22
10	25.09	.02	.30	.47	5.08	23.96	165.91
11	29.75	.13	.69	1.74	29.70	26.47	140.06
12	25.61	.30	.05	.05	3.60	10.56	183.63
13	29.76	.01	.85	.15	21.51	7.86	183.00
14	11.02	.57	1.14	.87	14.07	8.71	215.77
15	29.55	1.46	.03	.04	14.46	9.46	172.09
16	29.88	.01	5.43	.22	3.28	28.90	147.76
17	28.88	4.21	6.95	.31	24.05	14.94	125.69
18	23.81	2.38	1.93	.411	19.65	14.28	155.54
19	29.33	.81	1.84	.02	8.20	20.56	147.41
20	29.31	6.58	.45	0	4.40	18.68	150.97
21	29.89	−1.22	.65	0	13.44	23.44	118.69
22	2.59	5.85	2.13	0	9.53	6.20	137.25
23	27.52	4.72	.20	0	26.39	11.89	51.98
24	3.33	3.45	.48	0	13.71	6.95	57.07

Table 3
The results of power generation and storage planning in the microgrid for case 6.

Hour	Grid (kW)	Battery (kW)	Wind Turbine (kW)	Photovoltaic (kW)	Fuel cell (kW)	Micro turbine (kW)	Diesel generator (kW)
1	−29.87	−8.27	0	0	21.52	8.28	62.22
2	−29.87	12.87	0	0	29.87	16.31	40.12
3	−29.87	−29.64	.06	0	15.60	26.55	77.25
4	−29.87	5.39	.23	0	3.53	18.69	57.71
5	−29.87	2.24	2.41	0	4.49	7.96	46.87
6	−29.87	4.27	.71	0.41	17.66	9.21	30.92
7	−29.87	−.48	1.07	1.95	28.83	29.81	33.25
8	8.43	−25.70	1.43	4.61	29.86	29.87	116.54
9	29.87	20.27	1.84	6.60	19.62	29.03	97.98
10	−8.34	−29.87	2.34	1.98	29.87	21.28	198.77
11	−10.34	11.22	2.97	13.06	29.73	29.87	148.23
12	−25.49	26.75	3.76	13.88	29.87	21.61	140.87
13	−29.87	−6.92	4.72	12.55	28.89	26.24	203.91
14	−12.48	11.87	5.97	9.55	28.47	29.87	164.80
15	−7.60	−28.73	6.84	6.69	5.31	6.37	226.09
16	29.69	29.87	7.90	3.69	29.77	29.87	8267/73
17	−28.37	−29.64	8.88	2.48	28.87	25.08	190.73
18	−22.57	25.69	91.75	1.45	13.25	24.07	135.73
19	1.14	−18.76	10.70	.23	29.86	15.07	158.90
20	14.88	28.15	11.56	0	5.11	8.57	139.67
21	−29.87	−15.10	12.43	0	29.70	29.87	16.08
22	−29.87	15.57	12.93	0	29.86	26.50	105.87
23	−24.24	−9.49	14.10	0	3.71	20.88	111.87
24	11.23	17.73	11.23	0	20.39	11.78	32.89

(generation power) and discrete variables (battery charge and discharge states). It was also observed that the operating and pollution costs of microgrids can be controlled and that a compromise can be made between the two in both grid-islanded and grid-connected modes. Moreover, it was found that, in grid-connected operation, the analyzed costs can be reduced to some extent. On the other hand, by applying uncertainty to the nominal value of some microgrid parameters, whose value is not exactly known in the natural state, an attempt was made to make the results of the proposed algorithm more realistic, and it was observed that the algorithm can obtain the optimal solution.

Authorship contributions

S. Mansouri: Conception and design of study, acquisition of data, Drafting the manuscript, revising the manuscript critically for important intellectual content. F. Zishan: Conception and design of study, acquisition of data, Drafting the manuscript, revising the manuscript critically for important intellectual content. O.D. Montoya: Conception and design of study, acquisition of data, Drafting the manuscript, revising the manuscript critically for important intellectual content. M. Azimizadeh: Conception and design of study, acquisition of data, Drafting the manuscript, revising the manuscript critically for important intellectual content. D.A. Giral-Ramírez: Conception and design of study, acquisition of data, Drafting the manuscript, revising the manuscript critically for important intellectual content.

Declaration of competing interest

The authors declare that they have no known competing financial interests or personal relationships that could have appeared to influence the work reported in this paper.

Data availability

Data will be made available on request.

Acknowledgements

All persons who have made substantial contributions to the work reported in the manuscript (e.g., technical help, writing and editing assistance, general support), but who do not meet the criteria for authorship, are named in the Acknowledgements and have given us their written permission to be named. If we have not included an Acknowledgements, then that indicates that we have not received substantial contributions from non-authors.

References

[1] L. Barelli, G. Bidini, F. Bonucci, A micro-grid operation analysis for cost-effective battery energy storage and RES plants integration, Energy 113 (2016), https://doi.org/10.1016/j.energy.2016.07.117.
[2] M.H. Moradi, M. Eskandari, S.M. Hosseinian, Operational strategy optimization in an optimal sized smart microgrid, IEEE Trans. Smart Grid 6 (Issue: 3) (May 2015), https://doi.org/10.1109/TSG.2014.2349795.
[3] K. Rahbar, J. Xu, R. Zhang, Real-time energy storage management for renewable integration in microgrid: an off-line optimization approach, IEEE Trans. Smart Grid 6 (Issue: 1) (January 2015), https://doi.org/10.1109/TSG.2014.2359004.
[4] YunfangXiea PengWena, AkbarTohidib LiminHuoa, '', Optimal and stochastic performance of an energy hub-based microgrid consisting of a solar-powered compressed-air energy storage system and cooling storage system by modified grasshopper optimization algorithm, Int. J. Hydrogen Energy 47 (Issue 27) (29 March 2022), https://doi.org/10.1016/j.ijhydene.2022.02.081.
[5] Kaiye Gao, Tianshi Wang, Chenjing Han, Jinhao Xie, Ye Ma, Rui Peng, Open access review A review of optimization of microgrid operation, Energies 14 (10) (2021) 2842, https://doi.org/10.3390/en14102842.
[6] C. Gamarra, J.M. Guerrero, Computational optimization techniques applied to microgrids planning: a review, Renew. Sustain. Energy Rev. 48 (August 2015), https://doi.org/10.1016/j.rser.2015.04.025.
[7] CorinnaMöhrlen JieYan, MarkKelly TuhfeGöçmen, GregorGiebelc ArneWessel, Uncovering wind power forecasting uncertainty sources and their propagation through the whole modelling chain, Renew. Sustain. Energy Rev. 165 (September 2022), https://doi.org/10.1016/j.rser.2022.112519.
[8] N. Ganjei, F. Zishan, R. Alayi, H. Samadi, M. Jahangiri, R. Kumar, A. Mohammadian, Designing and sensitivity analysis of an off-grid hybrid wind-solar power plant with diesel generator and battery backup for the rural area in Iran, J. Eng. 2022 (2022), https://doi.org/10.1155/2022/4966761.
[9] T.A. Nguyen, M. Crow, Stochastic optimization of renewable-based microgrid operation incorporating battery operating cost, IEEE Trans. Power Syst. 31 (Issue: 3) (May 2016), https://doi.org/10.1109/TPWRS.2015.2455491.
[10] Sim Wai Sheng, Yip Sook Yee, Jee Wong, Keen Raymond, Economic Dispatch of Micro-grid Considering Electric Vehicles, in: 11th IEEE International Conference on Control System, Computing and Engineering (ICCSCE), 2021, https://doi.org/10.1109/ICCSCE52189.2021.9530948.
[11] T. Nsilulu, C. MbunguabRamesh, M. BansalbRaj, '', A dynamic energy management system using smart metering, Appl. Energy 280 (2020), https://doi.org/10.1016/j.apenergy.2020.115990, 15 December.
[12] V.N. Coelho, I.M. Coelho, B.N. Coelho, M.W. Cohen, A.J. Reis, S.M. Silva, M. J. Souza, P.J. Fleming, F.G. Guimarães, Multi-objective energy storage power dispatching using plug-in vehicles in a smart-microgrid, Renew. Energy 89 (2016), https://doi.org/10.1016/j.renene.2015.11.084. April.

[13] R. Rigo-Mariani, B. Sareni, X. Roboam, Integrated optimal design of a smart microgrid with storage, IEEE Trans. Smart Grid 8 (Issue: 4) (July 2017), https://doi.org/10.1109/TSG.2015.2507131.
[14] F. Zishan, E. Akbari, O.D. Montoya, D.A. Giral-Ramírez, A.M. Nivia-Vargas, Electricity retail market and accountability-based strategic bidding model with short-term energy storage considering the uncertainty of consumer demand response, Res. Eng. (2022 Oct 3), 100679, https://doi.org/10.1016/j.rineng.2022.100679.
[15] S. Kakran, S. Chanana, Smart operations of smart grids integrated with distributed generation: a review, Renew. Sustain. Energy Rev. 81 (January 2018), https://doi.org/10.1016/j.rser.2017.07.045. Part 1.
[16] H. Alharbi, K. Bhattacharya, Stochastic optimal planning of battery energy storage systems for isolated microgrids, IEEE Trans. Sustain. Energy 9 (Issue: 1) (January 2018), https://doi.org/10.1109/TSTE.2017.2724514.
[17] M. Quashie, C. Marnay, F. Bouffard, G. Joós, Optimal planning of microgrid power and operating reserve capacity, Appl. Energy 210 (2018), https://doi.org/10.1016/j.apenergy.2017.08.015, 15 January.
[18] Mohammad Ghiasi, Taher Niknam, Moslem Dehghani, Optimal multi-operation energy management in smart microgrids in the presence of RESs based on multi-objective improved DE algorithm: cost-emission based optimization, Appl. Sci. 11 (8) (2021) 3661, https://doi.org/10.3390/app11083661.
[19] G. Carpinelli, F. Mottola, D. Proto, A. Russo, A multi-objective approach for microgrid scheduling, IEEE Trans. Smart Grid 8 (Issue: 5) (September 2017), https://doi.org/10.1109/TSG.2016.2516256.
[20] X. Gong, F. Dong, M.A. Mohamed, O.M. Abdalla, Z.M. Ali, A secured energy management architecture for smart hybrid microgrids considering PEM-fuel cell and electric vehicles, IEEE Access 8 (2020), https://doi.org/10.1109/ACCESS.2020.2978789.
[21] J.D. Lara, D.E. Olivares, C.A. Canizares, Robust energy management of isolated microgrids, IEEE Systems Journal 13 (Issue: 1) (March 2019), https://doi.org/10.1109/JSYST.2018.2828838.
[22] E. Foruzan, L. Soh, S. Asgarpoor, Reinforcement learning approach for optimal distributed energy management in a microgrid, IEEE Trans. Power Syst. 33 (Issue: 5) (September 2018), https://doi.org/10.1109/TPWRS.2018.2823641.
[23] J. Wu, X. Xing, X. Liu, J.M. Guerrero, Z. Chen, Energy management strategy for grid-tied microgrids considering the energy storage efficiency, IEEE Trans. Ind. Electron. 65 (Issue: 12) (December 2018), https://doi.org/10.1109/TIE.2018.2818660.
[24] D. Romero-Quete, C.A. Cañizares, An affine arithmetic-based energy management system for isolated microgrids, IEEE Transactions on Smart Grid 10 (Issue: 3) (May 2019), https://doi.org/10.1109/TSG.2018.2816403.
[25] J. Montano, O.D. Garzón, A.A.R. Muñoz, L.F. Grisales-Noreña, O.D. Montoya, Application of the arithmetic optimization algorithm to solve the optimal power flow problem in direct current networks, Res. Eng. 16 (2022), 100654, https://doi.org/10.1016/j.rineng.2022.100654.
[26] G.S. Mohammed, S. Al-Janabi, An innovative synthesis of optimization techniques (FDIRE-GSK) for generation electrical renewable energy from natural resources, Res. Eng. 16 (2022), 100637, https://doi.org/10.1016/j.rineng.2022.100637.
[27] B. Raillani, D. Chaatouf, M. Salhi, A. Bria, S. Amraqui, A. Mezrhab, The effectiveness of the wind barrier in mitigating soiling of a ground-mounted photovoltaic panel at different angles and particle injection heights, Res. Eng. 16 (2022), 100774, https://doi.org/10.1016/j.rineng.2022.100774.
[28] M. Sundararaj, N. Rajamurugu, J. Anbarasi, S. Yaknesh, R. Sathyamurthy, Parametric optimization of novel solar chimney power plant using response surface methodology, Res. Eng. 16 (2022), 100633, https://doi.org/10.1016/j.rineng.2022.100633.
[29] D. Wang, J. Qiu, L. Reedman, K. Meng, L.L. Lai, Two-stage energy management for networked microgrids with high renewable penetration, Appl. Energy 226 (2018), https://doi.org/10.1016/j.apenergy.2018.05.112, 15 September.
[30] S. Nikkhah, A. Rabiee, Multi-objective stochastic model for joint optimal allocation of DG units and network reconfiguration from DG owner's and DisCo's perspectives, Renew. Energy 132 (March 2019), https://doi.org/10.1016/j.renene.2018.08.032.
[31] R. Aboli, M. Ramezani, H. Falaghi, Joint optimization of day-ahead and uncertain near real-time operation of microgrids, Int. J. Electr. Power Energy Syst. 107 (May 2019), https://doi.org/10.1016/j.ijepes.2018.10.032.
[32] Y. Zheng, B.M. Jenkins, K. Kornbluth, A. Kendall, C. Træholt, Optimization of a biomass-integrated renewable energy microgrid with demand side management under uncertainty, Appl. Energy 230 (2018), https://doi.org/10.1016/j.apenergy.2018.09.015, 15 November.
[33] R. Alayi, F. Zishan, M. Mohkam, S. Hoseinzadeh, S. Memon, D.A. Garcia, A sustainable energy distribution configuration for microgrids integrated to the national grid using back-to-back converters in a renewable power system, Electronics 10 (15) (2021), https://doi.org/10.3390/electronics10151826, 1826.1826.
[34] E. Akbari, N. Shafaghatian, F. Zishan, O.D. Montoya, D.A. Giral-Ramírez, Optimized two-level control of islanded microgrids to reduce fluctuations, IEEE Access (2022), https://doi.org/10.1109/ACCESS.2022.3203730.
[35] ChenLi, GuoChen, GaoqiLiang, Integrated optimization algorithm: a metaheuristic approach for complicated optimization, Inf. Sci. 586 (March 2022), https://doi.org/10.1016/j.ins.2021.11.043.
[36] MauroCastelli, et al., Salp swarm optimization: a critical review, Expert Syst. Appl. 189 (March 2022) 1, https://doi.org/10.1016/j.eswa.2021.116029. Cite.
[37] L. Tightiz, S. Mansouri, F. Zishan, J. Yoo, N. Shafaghatian, Maximum power point tracking for photovoltaic systems operating under partially shaded conditions using SALP swarm algorithm, Energies 15 (21) (2022) 8210, https://doi.org/10.3390/en15218210.
[38] S. Rajamand, '', Effect of demand response program of loads in cost optimisation of microgrid considering uncertain parameters in PV/WT ,market price and load demand, Energy 194 (March 2020) 1, https://doi.org/10.1016/j.energy.2020.116917.
[39] JiyuXia BowenZhou, Multi-time scale optimal scheduling model for active distribution grid with desalination loads considering uncertainty of demand response, Desalination 517 (1) (December 2021), https://doi.org/10.1016/j.desal.2021.115262.
[40] YuWang, YuFu, HaiyangLin, Uncertainty modeling of household appliance loads for smart energy management, Energy Rep. 8 (Supplement 1) (April 2022), https://doi.org/10.1016/j.egyr.2021.11.097.
[41] Jose M. Pinto, Ignacio E. Grossmann, Sumit Mitra, Optimal multi-scale capacity planning for power-intensive continuous processes under time-sensitive electricity prices and demand uncertainty. Part I: modeling, Comput. Chem. Eng. 65 (4 June 2014), https://doi.org/10.1016/j.compchemeng.2014.01.016.
[42] A.A. Moghaddam, A. Seifi, T. Niknam, M.R.A. Pahlavani, Multi-objective operation management of a renewable MG (micro-grid) with back-up micro-turbine/fuel cell/battery hybrid power source, Energy 36 (11) (2011) 6490–6507, https://doi.org/10.1016/j.energy.2011.09.017.